

Thermal rectification phenomenon on suspended half-meshed graphene devices

Fayong Liu¹, Manoharan Muruganathan¹, Shinichi Ogawa², Yukinori Morita², Zhongwang Wang¹,
Jiayu Guo¹, Mayeesha Haque¹, Marek Schmidt¹, Hiroshi Mizuta^{1,3}

¹ Japan Advanced Institute of Science and Technology, Japan. [E-mail: fayong@jaist.ac.jp](mailto:fayong@jaist.ac.jp)

² National Institute of Advanced Industrial Science and Technology, Japan. ³ Hitachi Cambridge Laboratory, United Kingdom

Abstract — We report on the successful fabrication of suspended half-meshed graphene devices and the observation of the thermal rectification phenomenon at 150 – 250 K. The nanomesh area is patterned by drilling 6nm-diameter-nanopore array on the suspended graphene nanoribbon with helium ion beam milling (HIBM) technique. By decreasing the environmental base temperature, the thermal rectification ratio is enhanced.

1. Introduction

The thermal rectification phenomenon is a concept as same as the electrical diode, that the heat flux in one preferred direction is larger than the opposite direction [1]. Nowadays, the research interest is switched to nanomaterials rather than bulk materials. The two-dimensional materials such as monolayer graphene provide an ideal platform to modify the crystal structure at the atomic level, which leads the way to link the thermal conductivity with the lattice defects [2]. In the previous work, the thermal rectification based on suspended graphene has been reported by introducing asymmetric structure, deposition, and randomly large defects [3]. However, the experiment on graphene nanomesh (GNM) with periodic nanopores pattern on suspended graphene nanoribbon (GNR) for thermal rectification has not been reported. In this study, we introduce periodic sub-10 nm nanopores on suspended GNR by the helium ion beam milling (HIBM) technique. The thermal rectification was investigated at two different environmental-based temperatures.

2. Device fabrication

The schematic structure of the device is shown in Fig. 1. We introduced periodic nanopores in the right half of the suspended GNR. The fabrication details have been demonstrated in our previous work [4]. In short, the process was started with transferring the chemical-vapor-deposition (CVD) graphene on a p-doped Si substrate with a thermal SiO₂ layer (285 nm). Then the first electrode layer (80/5 nm Au/Cr) was patterned to achieve good adhesion with the substrate. The underneath graphene was removed before depositing the metal layers (Fig. 2a). The second electrode layer (70/5 nm Au/Cr) was patterned to make good contact between the previous metal layer and graphene (Fig. 2b). Subsequently, GNR was formed by electron beam lithography (EBL) patterning with hydrogen silsesquioxane (HSQ) and plasma etching (Fig. 2c). In the last step, the GNR was suspended by buffered hydrofluoric (BHF) etching (Fig. 2d). By controlling the dwell time of the beam during the HIBM, the diameter of nanopores were fixed at about 6nm (Fig. 5). In order to investigate the impact weight of both the GNR and GNM parts during the thermal transport, we kept the same length of the GNR and GNM parts (Fig. 4).

3. Measurement results

The device was measured in a high vacuum cryostat. A “hot wire” method was used to evaluate the thermal transport through the suspended graphene [5]. We compared the temperature difference (ΔT) of the heater between “no bridge” (Fig. 6) and “graphene bridge” (Fig. 7) conditions with the same heating power. Then the heat flow in one direction

could be estimated. As the gold nanowires on both sides are symmetrical (Fig. 3), we can reverse the roles of heater and heat sink to evaluate the heat flow in both directions. The selected device in Fig. 4 is 500 nm long and 1.2 μm wide with 20 nm-pitch (center to center) nanopore array on half of the device. To check electron properties, $I_D - V_D$ characteristics (Fig. 8) were measured at different temperatures in both current directions. Fig. 9 showed that the conductance from different directions was the same from 20 K to 300 K. So that the electron contribution to the thermal conductivity is the same from two directions. We measured the ΔT both from Left to Right ($L > R$, ΔT_L) and Right to Left ($R > L$, ΔT_R) at 150 K and 250 K environmental base temperatures (Fig. 10). It shows that the heat flow from the GNM side is much larger than that from the GNR side at 150K. However, the thermal rectification ratio is decreased significantly at 250 K. The physical mechanism is explained in Fig. 11 [6-7]. The solid lines represent the temperature-dependent thermal conductivity (κ) of the total suspended device from one direction at different temperatures. Due to the Umklapp process, the total thermal conductivity of the pink solid line is much larger than the bright blue solid line at 150 K. However, because of the saturate trend of κ for GNR at higher temperatures, it leads to the shrink of the thermal rectification ratio at 250 K. It noteworthy that the ΔT_L is increased at a higher temperature, which decreases the thermal rectification ratio. That means the total thermal conductivity of the blue solid line should be larger than the bright blue solid line. It implies that the increment of κ for GNM should be larger than the decrement of κ for GNR in the high-temperature region. In this case, systematically modifying κ for GNM to be non-temperature dependence is essential to improve the thermal rectification ratio at high temperatures.

4. Summary

We successfully patterned GNM on a half area of suspended GNRs with the HIBM technique. By using the “hot wire” method, we observed the thermal rectification phenomenon at 150 K and 250 K base temperatures. The device achieved a higher thermal rectification ratio at 150 K. Due to the saturation of the Umklapp process and the temperature dependence of the κ for GNM, the ratio was significantly decreased in the higher temperature region.

Acknowledgments

The authors acknowledge T. Iijima and H. Ota for the usage of the HIBM at the AIST SCR station for the helium ion irradiations. This work was supported by the Grant-in-Aid for Scientific Research No. 18H03861, 19H05520 from the Japan Society for the Promotion of Science (JSPS).

References

- [1] R.R Somers *et al.*, *AIAA J.* (1987) **25**, 620-621.
- [2] A. Arora, *et al.*, *Phys. Rev. B*, (2017) **96**, 165419.
- [3] H. Wang, *et al.*, *Nat. Commun.*, (2017) **8**, 15843.
- [4] F. Liu, *et al.*, *Micromachines*, (2020) **11**, 387.
- [5] M. Fujii, *et al.*, *Phys. Rev. Lett.*, (2005) **95**, 065502.
- [6] D.L. Nika, *et al.*, *Phys.: Condens. Matter*, (2012) **24**, 233203.
- [7] L. Yang, *et al.*, *Int. J. heat mass tran.*, (2015) **91**, 428-432.

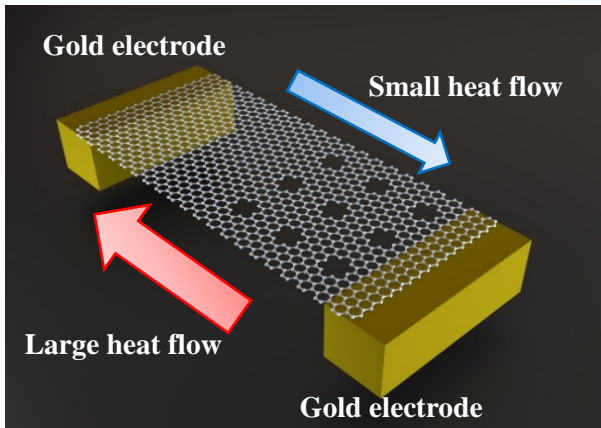


Fig. 1: Schematic illustration of the asymmetric thermal properties on the half-meshed suspended graphene.

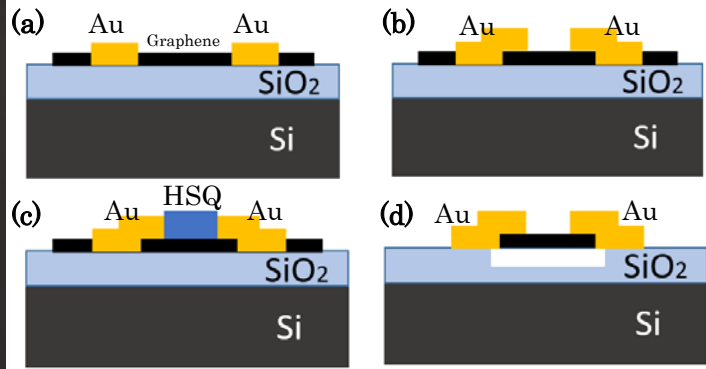


Fig. 2: Main fabrication steps. (a) the first electrode layer patterning after CVD graphene transfer. (b) the second electrode layer patterning. (c) GNR patterning with HSQ. (d) suspending the GNR by wet etching after plasma etching.

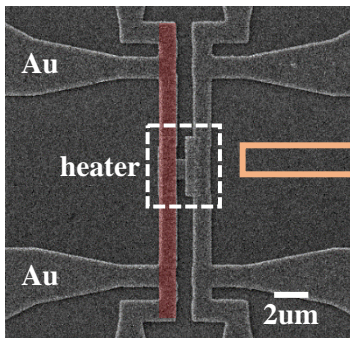


Fig. 3: Helium ion beam microscopy image of the device structure.

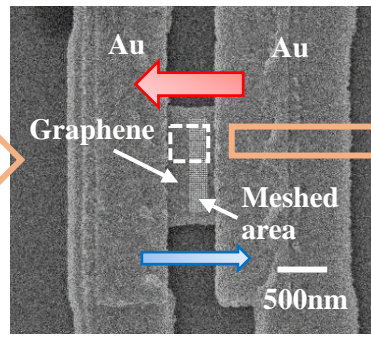


Fig. 4: Helium ion beam microscopy image of the suspended part.

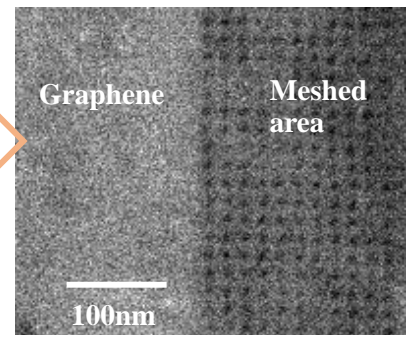


Fig. 5: Helium ion beam microscopy image of the half-meshed area

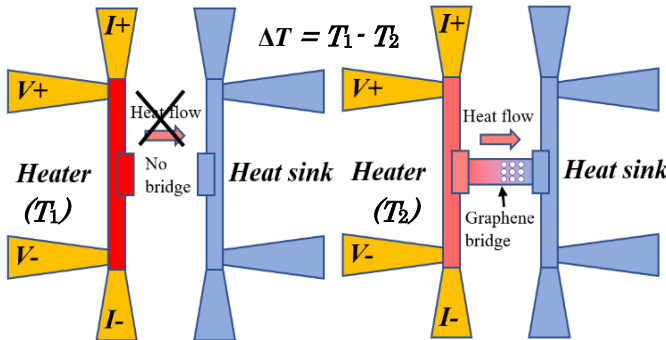


Fig. 6: "no bridge" condition in the "hot wire" method. Fig. 7: "graphene bridge" condition in the "hot wire" method.

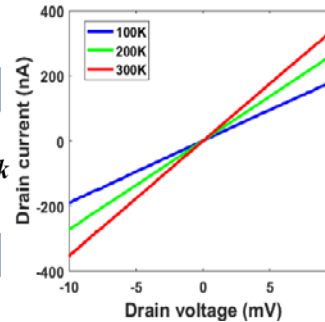


Fig. 8: $I_D - V_D$ at different temperature from one direction

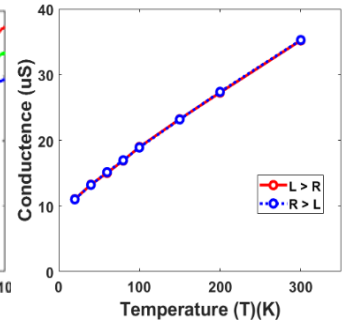


Fig. 9: temperature dependence from 20K to 300K from two directions

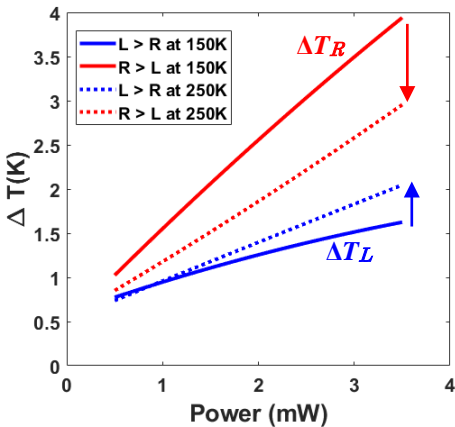


Fig. 10: ΔT measurement results at 150 K and 250 K base temperatures.

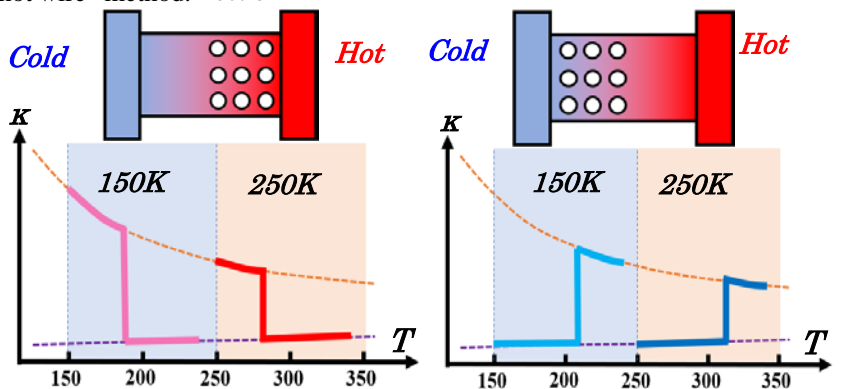


Fig. 11: Explanation of the physical mechanism. In the $\kappa-T$ curves, the orange and purple dashed lines represent the temperature dependence of thermal conductivity for GNR and GNM. The pink and red solid lines are for heating from GNM side at 150 K and 250K. The bright blue and blue solid line are for heating from GNR side at 150 K and 250K.